NREL
NATIONAL RENEWABLE ENERGY LABORATORY

Combining Droop Curve Concepts with Control Systems for Wind Turbine Active Power Control

Preprint

A. Buckspan, J. Aho, and L. Pao
University of Colorado at Boulder

P. Fleming
National Renewable Energy Laboratory

Y. Jeong
Colorado School of Mines

To be presented at the IEEE Symposium on Power Electronics and Machines in Wind Applications
Denver, Colorado
July 16-18, 2012

Conference Paper
NREL/CP-5000-55211
June 2012

Contract No. DE-AC36-08GO28308

Combining Droop Curve Concepts with Control Systems for Wind Turbine Active Power Control

Andrew Buckspan, Jacob Aho, Paul Fleming, Yunho Jeong, Lucy Pao

***Abstract*—Wind energy is becoming a larger portion of the global energy portfolio, and wind penetration has increased dramatically in certain regions of the world. This increasing wind penetration has driven the need for wind turbines to provide active power control (APC) services to the local utility grid, as wind turbines do not intrinsically provide frequency regulation services that are common with traditional generators. Large scale wind turbines are typically decoupled from the utility grid via power electronics, which allows the turbines to synthesize APC commands via control of the generator torque and blade pitch commands. Consequently, the APC services provided by a wind turbine can be more flexible than those provided by conventional generators.**

This paper focuses on the development and implementation of both static and dynamic droop curves to measure grid frequency and output delta power reference signals to a novel power set point tracking control system. The combined droop curve and power tracking controller is simulated and comparisons are made between simulations using various droop curve parameters and stochastic wind conditions. The tradeoffs involved with aggressive response to frequency events are analyzed. At the turbine level, simulations are performed to analyze induced structural loads. At the grid level, simulations test a wind plant's response to a dip in grid frequency.

NOMENCLATURE

β	blade pitch angle
Ω_g	generator speed
τ_g	generator torque
AGC	automatic generation control
APC	active power control
BPF	band-pass filter
$CART3$	3-bladed Controls Advanced Research Turbine
DDC	dynamic droop curve
DEL	damage equivalent load
$ERCOT$	Electric Reliability Council of Texas
LPF	low-pass filter
$NREL$	National Renewable Energy Laboratory
PI	proportional-integral
RL	rate limit
$ROCOF$	rate of change of frequency
SDC	static droop curve
TSO	transmission systems operator

Andrew Buckspan is a doctoral student in the Dept. of Electrical, Computer, and Energy Engineering, University of Colorado, Boulder, e-mail: andrew.buckspan@colorado.edu.

Jacob Aho is a doctoral student in the Dept. of Electrical, Computer, and Energy Engineering, University of Colorado, Boulder, e-mail: jacob.aho@colorado.edu.

Paul Fleming is a research engineer at the National Wind Technology Center, Boulder, e-mail: paul.fleming@nrel.gov.

Yunho Jeong was a graduate student in the Division of Engineering, Colorado School of Mines, Golden, e-mail: yunho3600@gmail.com.

Lucy Pao is the Richard & Joy Dorf Professor in the Dept. of Electrical, Computer, and Energy Engineering, University of Colorado, Boulder, e-mail: pao@colorado.edu

This paper is produced as part of the NREL Active Power Control from Wind Power Project. This work was supported in part by the U.S. Department of Energy's Office of Energy Efficiency and Renewable Energy Wind and Hydropower Technologies Program and also by a University of Colorado Boulder College of Engineering and Applied Science Dean's Graduate Assistantship.

I. INTRODUCTION

Wind energy is a growing renewable energy technology, with a 27.7% mean annual growth rate in global installed capacity over the past decade [1]. While capacity levels in 2010 had wind energy providing only 2.5% of the global electrical energy supply, countries such as Denmark, Portugal, Spain, and Germany produced 21%, 18%, 16%, and 9% of their annual energy from wind, respectively [1]. The higher wind penetrations in these countries have driven the interest in wind energy providing active power control (APC) services to help stabilize grid frequency.

Transmission systems operators (TSOs) require conventional utilities to provide frequency regulation services in order to maintain the necessary balance between generation and load, which in turn regulates grid frequency. Conventionally, grid frequency response to a large disturbance is divided into separate control regimes: inertial, primary frequency response, and secondary frequency response or automatic generation control (AGC). The various phases of grid frequency response can be seen in Fig. 1. These classifications are based on methods for providing each service with conventional generators: synchronous generator inertia for inertial response, turbine governors for primary response, and finally output control responding to system operator power level demands for AGC response. For further information and exact definitions of inertial, primary, and secondary response, see [2] and [3].

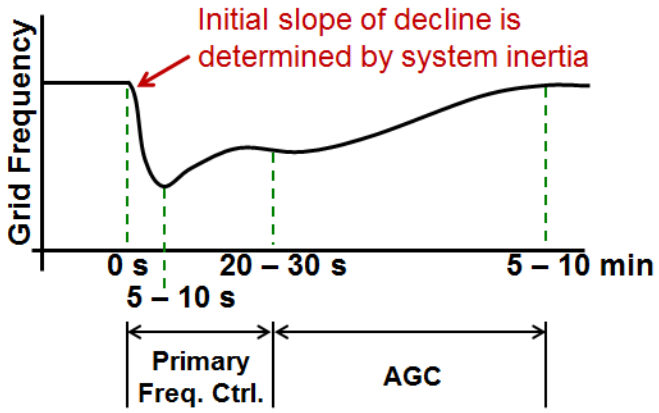

Fig. 1. Inertial, primary frequency, and secondary (AGC) frequency response phases. Figure reproduced from image provided by Pouyan Pourbeik of EPRI.

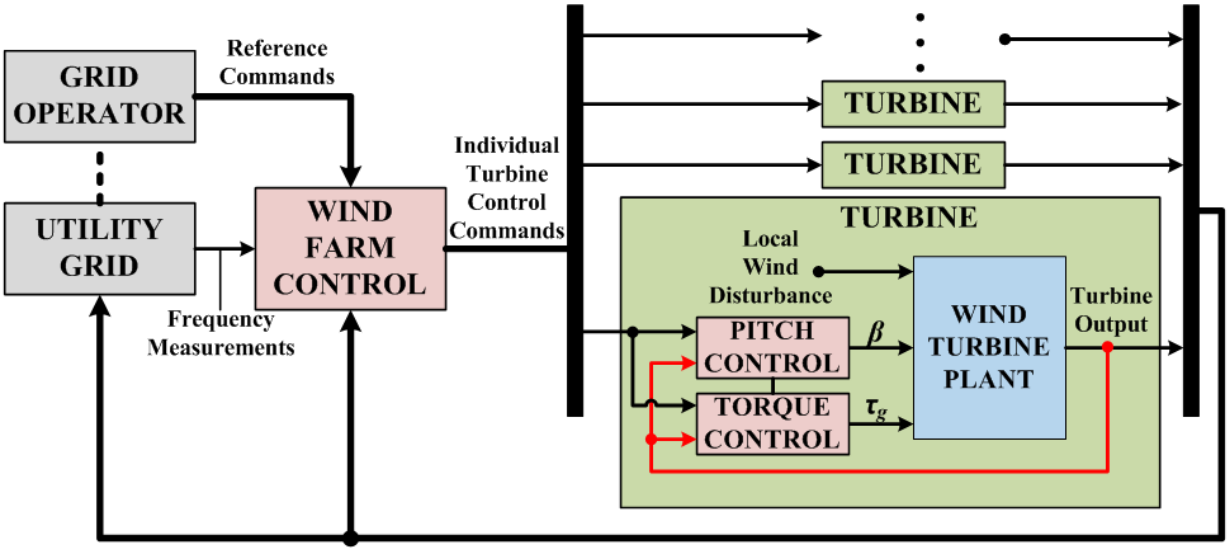

Fig. 2. A block diagram showing the general interconnection for APC commands. The wind plant controller can measure the frequency of the utility grid and receive an AGC power command signal from the grid operator and in turn produce a power reference for each turbine in the wind plant. From [4] with permission.

Wind power has not historically been required to provide APC services, as most modern wind turbines do not intrinsically provide any of the frequency regulation services that are available with conventional generators because utility-scale wind turbines are usually decoupled from the grid via their power electronics. However, new requirements and regulations put on wind plants by TSOs in the aforementioned countries have lead to new research and development to enable wind turbines to meet APC requirements. These regulations require that (1) new wind plants provide an inertial response when grid frequency deviates from the normal operating point and (2) wind plants meet a power set point provided by the TSO at a specified rate of change [5]-[9]. The interconnection of a wind plant controller with the utility grid, TSO, and individual turbines can be seen in Fig. 2. The new TSO requirements have forced manufacturers to meet these minimum requirements to provide inertial and AGC response.

This paper provides an overview of prior research in wind turbine primary response and describes a new methodology of using droop curve concepts with a novel wind turbine control system. Droop curves typically relate fluctuations in grid frequency to a corresponding change in power in a governor for a conventional synchronous generator. Augmenting a wind turbine control system designed to modify active power output with a droop curve can allow for participation in primary frequency response, as the APC system can automatically respond to changes in grid frequency in addition to active power set points requested by the grid operator. This paper focuses on analyzing the costs and benefits of using droop curves with various parameters on a single turbine, as well as on the utility grid as a whole.

The paper is organized as follows: Section II provides an overview of previous relevant work on APC of wind turbines to provide primary frequency response. Section III develops the combined droop curve and novel active power control methodology. Section IV presents selected simulation results using the droop curve augmented controller. Finally, Section V discusses future work and provides concluding comments.

II. Prior Relevant Research in Wind Turbine Primary Response

In this section, we present the most relevant prior research in implementing primary frequency control in wind turbines [10]-[15]. A feature common to these methodologies is the modification of generator torque based on measurements of the change in grid frequency and possibly the rate of change of grid frequency (ROCOF). In [10] and [11], the turbine is operated at a higher than optimal tip-speed ratio, allowing for an overhead power reserve. In the event that grid frequency deviates too far below nominal, generator torque is increased, extracting some inertia from the over-speeding rotor, and reducing the tip-speed ratio closer to optimal. A similar methodology is developed in [12]. Combined torque and blade pitch methodologies have also been developed, such as in [15]. Here, a proportional torque controller is used, where the gain can be variably adjusted according to grid frequency deviations. A blade pitch controller assists in primary response by decreasing pitch angle as necessary to ensure torque actuation during frequency transients does not cause large drops in mechanical power. In [13], a proportional-integral (PI) control loop generates a torque command that is used to operate the turbine on the optimal power-rotor speed trajectory. This control loop is augmented by loops that change the torque command proportionally to grid frequency deviations and ROCOF, with the former providing primary frequency control.

The use of droop curves to supplement wind turbine APC has also been investigated, such as in [13], [16], and [17]. In these studies, static linear droop curves, like those associated with governors for conventional generators, are used to generate a power reference based on frequency deviations, which is then an input to the control system. While [16] is generally more focused on voltage regulation through reactive power control, the use of droop curves in APC is briefly introduced. The use

of droop curves in frequency regulation is considered more thoroughly in [17]. Here, a supervisory controller generates a power set point, while deviations in grid frequency are passed through a droop curve, generating an offset in the power reference. In an under-frequency event, pitch angle is reduced to capture power that was previously being shed by the blades.

Simulations have been conducted to evaluate the performance of some of the proposed strategies for providing primary frequency response with wind turbines. In [13], two small-scale grid simulations were analyzed to determine the effect on grid frequency caused by losing a conventional generator. Primary frequency support was provided by the wind turbines in only one of the simulations. In a similar study [18], simulations analyzed an electric grid with varying levels of penetration by wind turbines with primary frequency control capabilities. Here, the grid was modeled as a single electrical bus, and the effect of loss of a generator on grid frequency was monitored. These simulations indicate that wind turbines can help arrest grid frequency dips and reduce maximum frequency deviations by participating in primary response. These simulations are, however, limited by their use of simplified wind turbine models. These simulations also neglect to analyze possible increases in turbine structural loads that can be induced when APC is employed.

III. Overview and Implementation of Droop Curves

In this section, we discuss a wind turbine controller designed for power set-point tracking combined with droop curves that generate the power reference commands.

A. Control System Description

The controller used in this study is adapted from one provided in [19], where a number of controllers were designed to implement APC on wind turbines by tracking a power reference signal provided to the turbine control system. The reference signal is generally an absolute AGC power reference signal [19]. The APC torque controller tracks a power reference for a given rotor speed by changing torque proportionally to the power set point but only works well in above-rated wind speed when the blade pitch controller is regulating rotor speed. The APC pitch controller is a gain-scheduled PI controller, similar to the one described in [20], which uses the power reference command to determine the speed set point along the baseline torque-speed trajectory, as seen in Fig. 3.

The APC torque and pitch controllers are combined in [19] using various methods, with the most promising method using filters to divide the control action between the torque and pitch controllers. The power reference signal is band-pass filtered and delivered to the torque controller, as the APC torque controller offers much faster response to changing power reference than does the pitch controller. The power reference input is low-pass filtered before being passed to the APC pitch controller, as the blade pitch motor cannot actuate as quickly as the torque can but performs much better in regulating the steady-state power output. This methodology is the basis of the APC controllers developed for this study.

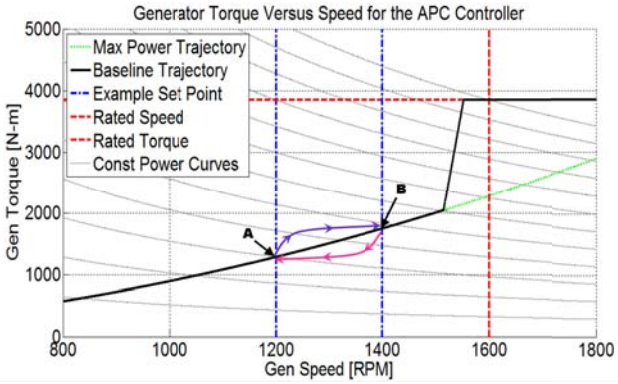

Fig. 3. The baseline torque-speed trajectory for the turbine simulated in this study is shown with an overlay of constant power curves. The APC controller used determines the speed set point for the blade pitch controller to be the point on the baseline trajectory that intersects the desired power reference. The torque controller will nominally follow the baseline trajectory but will track band-pass filtered power reference fluctuations given the speed set point.

B. Droop Curve Description

The previously described controller was originally designed to provide secondary services by tracking an AGC power reference signal. However, it can be adapted to participate in primary grid response if the power reference signal is augmented to respond to variations in grid frequency. This can be achieved through the use of a droop curve, which relates deviations in grid frequency to changes in power reference.

Droop curves are traditionally used to characterize the response of the governor of a synchronous generator to grid frequency deviations. These droop curves are parameterized based on their slope, usually given in percentage. For example, a governor with a 5% droop curve would vary the power output of the generator by 100% of rated power for a 5% deviation from nominal grid frequency. A deadband is often used to prevent the governor from actuating unnecessarily when small amplitude fluctuations in grid frequency are detected. Fig. 4 shows the static droop curves (SDCs) used in this study.

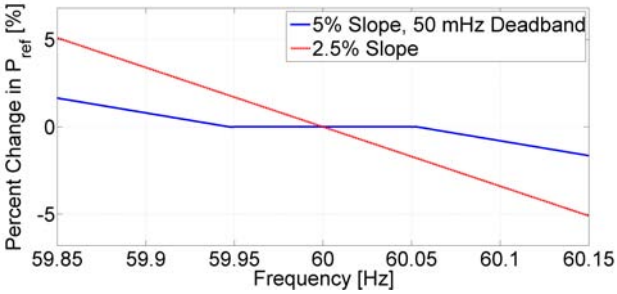

Fig. 4. The SDCs shown here are used in simulations both at the individual turbine and utility grid level.

Providing primary response using a droop curve differs from the methods described in Section II, as these methods treat frequency and ROCOF as direct control inputs. Using a droop curve to augment the existing APC controller simply modifies the power reference signal, allowing power reference to still be the only input into the control system. This means that the control system itself does not have to be redesigned or re-tuned to provide primary response capabilities. This is a potential advantage, as a great deal of work in industry, such as that

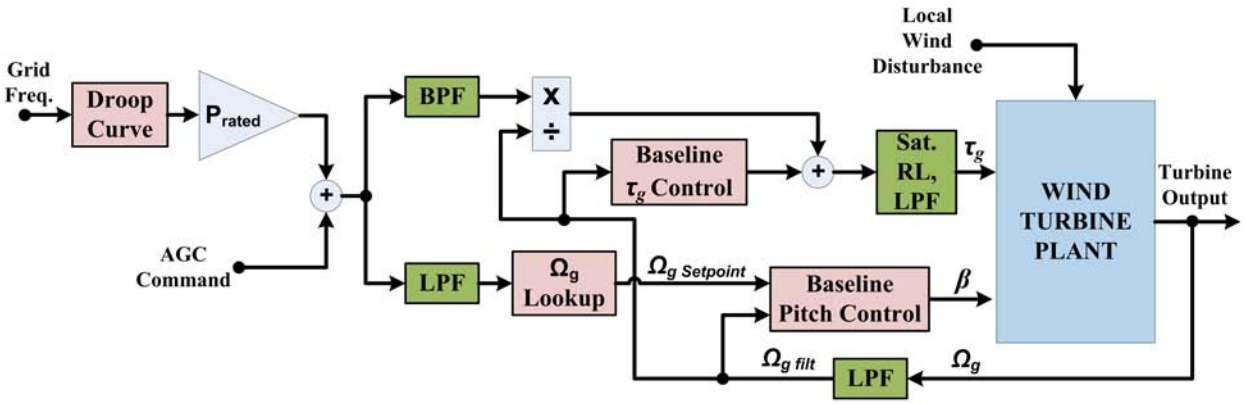

Fig. 5. A block diagram of the APC controller augmented with a droop curve to provide inertial/primary response. Features of note include the band-pass filtered (BPF) input into the torque controller, low pass filtered (LPF) input into the blade pitch controller, and saturation and rate limited (RL) torque input into the plant.

in [21] and [22], has been to develop APC systems that provide secondary regulation by tracking a reference power signal.

The use of droop curves to generate a power reference signal for a wind turbine or wind plant has a number of possible advantages over using frequency and ROCOF as direct inputs into the wind turbine APC system. For one, implementing a droop curve with a deadband can prevent the control system from persistantly actuating in reaction to small amplitude fluctuations in grid frequency. Additionally, droop curve slopes can be set at different values in different frequency regions. For example, the droop curve can be shaped so that it has a more aggressive slope for overfrequency events than underfrequency events.

Further, a wind turbine droop curve is implemented synthetically, and serves only to generate a power reference into the APC system. This differs from a traditional synchronous generator, where the droop curve characterizes the physical response of the governor. Therefore, droop curve characteristics can be dynamically changed online in response to ROCOF. For example, if a large ROCOF is detected, the droop curve slope can be increased and deadband decreased in anticipation of an underfrequency event. Dynamically shaping the droop curve can potentially allow for aggressive response to large changes in frequency, effectively adding extra inertial response, without inducing excessive loads on the turbine components.

The dynamic droop curves (DDCs) used in this study were set to have a nominal slope and deadband width, which was then changed to a more aggressive value if ROCOF exceeded a minimum threshold. At a maximum ROCOF, a maximum slope and minimum deadband width were reached, which would then be kept for increasing ROCOF. For ROCOF between the minimum and maximum thresholds, the droop curve characteristics were linearly interpolated between the nominal and most aggressive values. Further, droop curve "shaping" is only permitted when ROCOF and the frequency deviation have the same sign; that is, only if the frequency deviation is above nominal and ROCOF is serving to increase frequency or if the deviation is below nominal and ROCOF is serving to decrease frequency. The droop curves used in this study are summarized in Table I.

TABLE I
DROOP CURVE PARAMETERS

Droop Curve	Slope Range	Deadband Range	ROCOF Thresholds
SDC1	5%	50 mHz	n/a
SDC2	2.5%	0 mHz	n/a
DDC1	5-2.5%	50-0 mHz	5-10 mHz/sec
DDC2	5-2.5%	50-0 mHz	1-5 mHz/sec
DDC3	7.5-5%	50-0 mHz	5-10 mHz/sec

IV. SIMULATION RESULTS

A. Individual Turbine Simulation Results

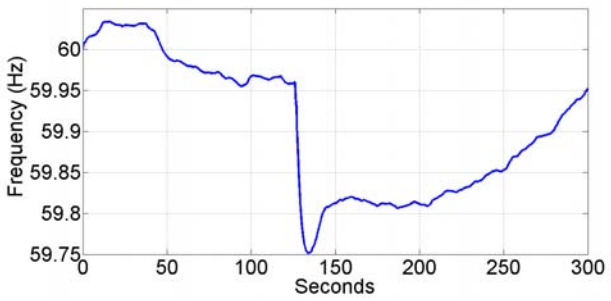

Fig. 6. This frequency event was measured on the ERCOT grid on Nov. 29, 2011. The total load on the grid was 30,071 MW. The frequency drops to 59.694 Hz after 1,365 MW of generating resource abruptly goes offline. Data courtesy of Vahan Gevorgian (NREL).

Simulations at the individual turbine and grid level were carried out to evaluate the performance of multiple droop curves combined with the controller described in Section III. The combined droop curve and APC system is depicted in Fig. 5. Individual turbine tests were carried out using the FAST wind turbine response simulation code developed by the National Renewable Energy Laboratory (NREL) [23]. The APC controller was augmented using the droop curves described in Table I. The simulations used five stochastic wind fields, each with a mean wind speed of 18 m/s, and results were averaged over the five simulations for each droop curve considered. Time series data from a frequency dip, measured during a generator fault on the Electric Reliability Council of Texas (ERCOT) grid, is passed through the static, linear droop curves shown in Fig. 4.

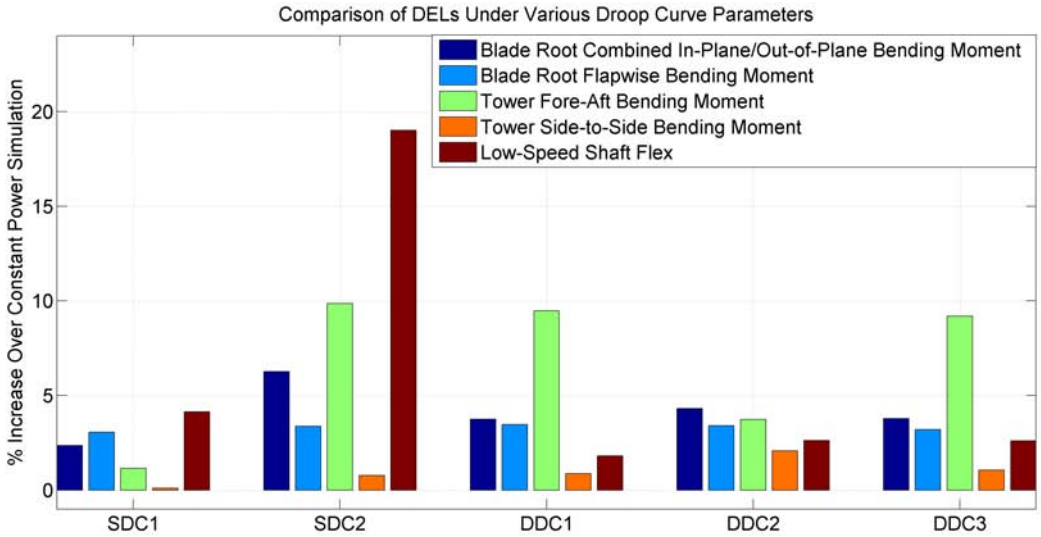

Fig. 7. The DELs induced during simulations with a stochastic wind field and the reference frequency input from Fig. 6.

This frequency dip is shown in Fig. 6. The effect of the droop curve and controller on the turbine was measured in terms of the damage equivalent loads (DELs) that were induced on the turbine components during the simulations, as seen in Fig. 7. A description of DELs can be found in [24].

As can be seen in Fig. 7, varying the parameters of the static droop curves affected the intensity of the induced structural loads. The baseline case is a constant power reference, which was set to 40% of rated power. Compared to this baseline, augmenting the power reference with a droop curve increases the structural loads on the turbine when using any of the droop curves. This is due to increased actuation of both the blade pitch and torque controllers in response to the rapidly changing power reference supplied by the droop curve in response to the variation in grid frequency. Further, the more aggressive SDC2 response to the frequency event, characterized by the 2.5% droop curve with no deadband, had the effect of increasing all of the measured DELs relative to SDC1, as the SDC2 droop curve causes the power reference to change more dramatically compared to the SDC1 case.

The effects on DELs of using the dynamic droop curves are more complex than those caused by the two static droop curves. Compared to the SDC1 case, increases in both of the tower bending moments and both of the blade root bending moments can be seen in all of the DDC cases. The low-speed shaft flex is improved in all of the three DDC cases. Further, with the exception of the tower fore aft-bending moment, the DELs increased or were unchanged between the DDC1 and DDC2 cases, which indicates that decreasing ROCOF thresholds as a means to achieve more aggressive frequency can change induced structural loads. Additionally, the DDC3 case had similar DELs to those in the DDC1 case, with the exception of a slight increase in the low-speed shaft flex, which would indicate that changing the slope range does not have as a great of an effect as changing the ROCOF thresholds with the ROCOF ranges considered in this study.

The induced DELs caused by using the dynamic droop curves are also shown in comparison to the SDC2 curve simulation in Fig. 7. The SDC2 droop curve represents the worst case of induced structural loads in the static droop curve cases. It can be seen that, with the exception of the tower side-to-side bending moment in the DDC2 simulation, the dynamic droop curve cases resulted in generally lower DELs than this worst-case static droop curve simulation. Hence, the loads induced by dynamic droop curves are in a middle ground between the best and worst cases observed using only static droop curves.

B. Grid Simulation Results

It is also desirable to test out the effects of a droop curve in combination with a wind turbine APC system at the utility grid level. A simple simulation of a grid represented as a single bus was used to analyze the effects of the APC controller in coordination with conventional generation when there is a frequency event. The grid model used in this study has hydro, wind, reheat and non-reheat steam turbine plants producing 40%, 15%, 40%, and 5% of power, respectively. The models for the conventional units in this simulation are based on control diagrams that can be found in [25]. Fig. 8 shows the grid frequency for simulations where the non-reheat steam turbine (5%) abruptly goes offline at time t = 1000 seconds. In the ”no wind” case, the wind plant is replaced with a reheat steam turbine. It can be seen that when the wind plant is operating with its normal ‘baseline’ control system set to simply track a constant power reference, the frequency response is worse due to the reduced amount of conventional generation providing frequency response. It should be noted that this effect assumes that wind fully decommits another utility (a reheat steam turbine in this case), whereas [26] shows that in the case where some of the generators are derated rather than all decommitted, this effect is much more limited or possibly reversed.

The aforementioned APC system was simulated using the same droop curves used for the individual turbine simulations. It can be seen in Fig. 8 that the frequency response is affected when the APC system is augmented with the static droop curves. The smallest deviation from nominal frequency is achieved with the SDC2 case, but this also causes large, undesirable

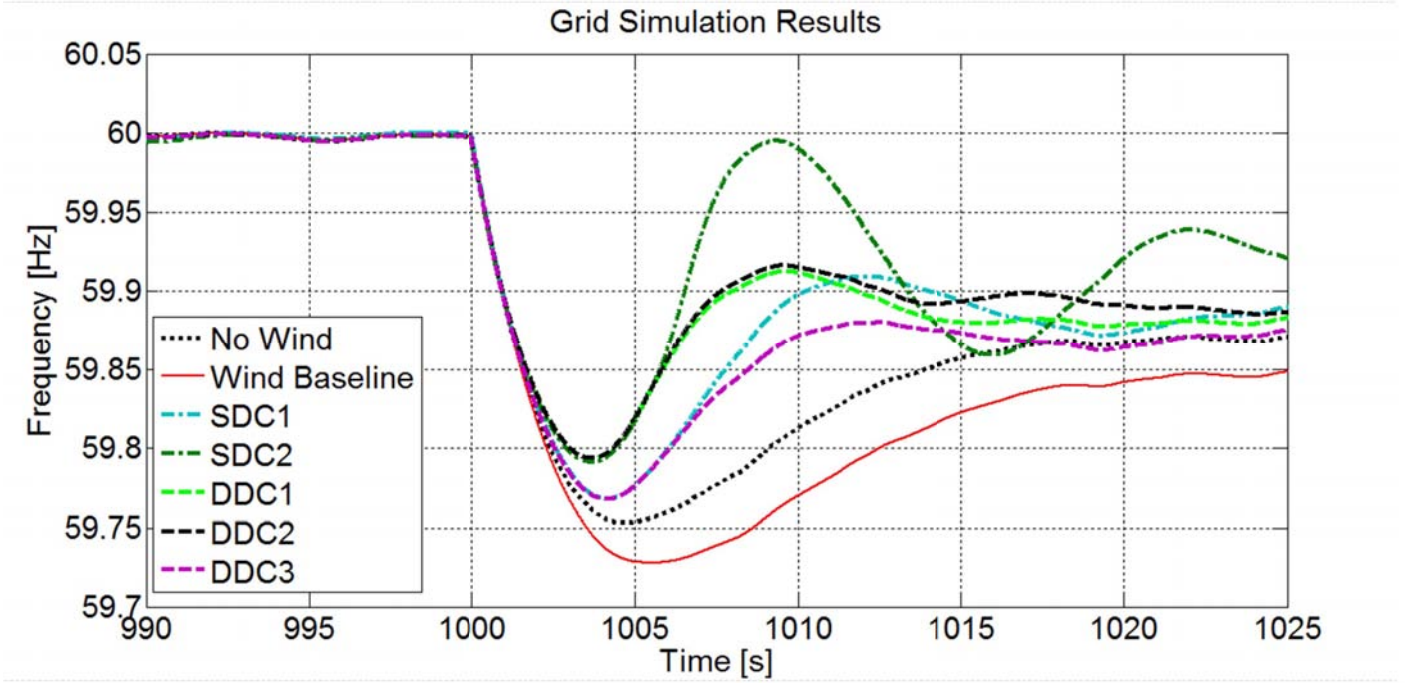

Fig. 8. Simulation results from a single bus grid. At 1000 seconds 5% of generating capacity goes offline. The system response with all conventional generation is compared to the cases when there is a wind plant at 15% penetration with a baseline control system or the droop curve and APC system configurations.

oscillations as frequency recovers to nominal. The SDC1 case results in improved frequency response over both the ”no wind” and baseline wind cases. At the nadir, the grid frequency has deviated further from nominal than in the SDC2 case, but there are no oscillations in the secondary response in the SDC1 case. It appears from these simulations that using a more aggressive droop curve can help improve the frequency nadir, but can also cause oscillations and grid instability, as well as increase loads on the turbine (as shown in Fig. 7). Hence, there is a level at which providing inertial/primary APC using static droop curves can be a detriment to both the grid and the individual turbines themselves.

Fig. 8 shows that the use of dynamic droop curves results in improved performance in all three cases over both the ”no wind” and baseline simulations. Additionally, in the DDC1 and DDC2 simulations, the grid frequency recovery is improved compared to the SDC1 simulation and is comparable to the initial recovery of the SDC2 simulation. In both cases, the frequency nadir occurs earlier and the maximum deviation from nominal frequency is reduced. An interesting result is that the DDC1 and DDC2 results in Fig. 8 are essentially indistinguishable until the secondary recovery phase. This is likely due to the fact that during the inertial phase, ROCOF is fairly high, and in both cases the maximum ROCOF threshold is reached fairly quickly, so the droop curve shaping ”saturates” quickly for both cases. The frequency makes a slight dip around 1010 seconds, and as the DDC2 case is more sensitive to low values of ROCOF than is the DDC1 case, this dip is smaller for the DDC2 simulation. Therefore the steady-state primary response frequency value is slightly higher than in the DDC1 simulation.

Another interesting feature is that both the DDC1 and DDC2 cases do not exhibit the large oscillations in grid frequency seen when an aggressive static droop curve is used. This is likely

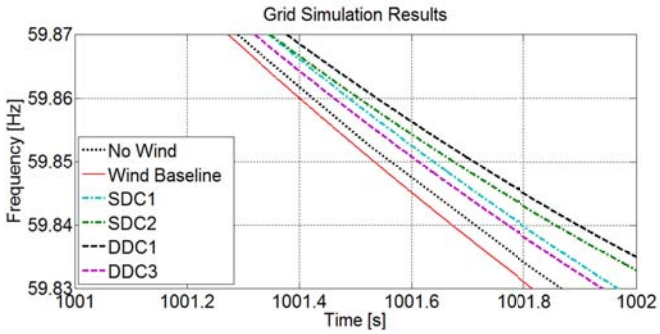

Fig. 9. Zoomed in plot showing ROCOF shortly after the grid fault occurs. Note that the DDC2 case is not shown, as at this time interval it is essentially identical to the DDC1 case.

due to the fact that the dynamic droop curve ‘shaping’ only occurs when the frequency is below nominal and ROCOF is negative. This causes an aggressive response in the first few seconds after the frequency event occurs, helping to arrest the decline in grid frequency. However, when the frequency starts to return to nominal, the response of the droop curve is not as aggressive. This is due to the fact that ROCOF is positive in this response phase, even though grid frequency is still below nominal.

Fig. 9 shows a zoomed-in view shortly after the frequency event occurs in the simulations to allow initial ROCOF to be seen more clearly. The DDC2 simulation is not shown, as it is again essentially indistinguishable from the DDC1 case in this time interval. The DDC1 case can be seen to have the shallowest initial ROCOF, while the wind baseline case has the steepest initial ROCOF. The DDC3 case has a steeper ROCOF than either of the SDC cases, but it is shallower than either the ”no wind” or baseline cases.

The improved grid response to loss of generation achieved

in the DDC1 and DDC2 cases comes at the cost of generally higher induced structural loads on the turbine compared to the SDC1 case. However, these dynamic droop curve cases offer a general decrease in structural loads when compared to the SDC2 simulation. Furthermore, the dynamic droop curve simulations do not create the same undesirable oscillations in grid frequency seen with this static droop curve simulation. These results demonstrate that a desirable middle ground of performance in terms of both structural loads and overall grid frequency performance can be achieved by using dynamic droop curves.

The results from the grid simulations are summarized in Table II. The frequencies are given in terms of percent deviation from 60 Hz, the time to the nadir is given as the elapsed time after the frequency event at time t=1000 seconds, and the steady-state frequency is given as the frequency 25 seconds after the frequency event occurs.

TABLE II
GRID SIMULATION RESULTS

Simulation Case	Nadir Freq.	Time to Nadir	Steady-State Freq.
No Wind	-0.417%	4.62 sec	-0.215%
Wind Baseline	-0.450%	5.51 sec	-0.253%
SDC1	-0.383%	4.28 sec	-0.183%
SDC2	-0.348%	3.70 sec	n/a
DDC1	-0.345%	3.70 sec	-0.198%
DDC2	-0.343%	3.70 sec	-0.198%
DDC3	-0.383%	4.17 sec	-0.208%

V. CONCLUSIONS AND FUTURE WORK

In this study, a previously designed APC system was augmented using various static and dynamic droop curves. The pre-existing APC system was designed to track an AGC power reference signal, and hence was only capable of providing secondary frequency response services. Through the use of a droop curve, this control system was able to provide inertial and primary frequency response as well. This provides a general methodology to adapt control systems designed for AGC power reference tracking to provide inertial and primary frequency response services.

The tradeoffs between aggressive frequency response and induced structural loads on an individual turbine were also analyzed. Several prior studies have simulated APC at the grid level, and one prior study simulated APC at the turbine level to analyze loads, but both have not previously been studied simultaneously. Using static droop curves, there is a clear tradeoff between using a more aggressive frequency response and increased loads. This tradeoff is most apparent when using a steeper droop curve slope.

Based on the grid simulations performed in Section IV-B, a relatively high penetration of wind not providing any APC capabilities has the effect of degrading overall grid frequency response, given that this wind plant entirely replaced another generating unit. Additionally, it is apparent that a noteable penetration of wind providing primary frequency response services can help improve overall grid recovery when a generator fault occurs. In all of the cases simulated using a droop curve to allow the APC system to participate in primary frequency response, overall frequency deviation was minimized, and the time to begin the return back to nominal frequency was reduced. However, grid instability was also observed when the wind plant response was too aggressive, and too much wind power was pushed onto the grid in response to a grid underfrequency event.

Two of the dynamic droop curves provided the best overall results. The concept of dynamically changing droop curve parameters online in response to grid ROCOF does not seem to appear in any existing literature on the subject, especially as it pertains to wind turbine APC. These dynamic droop curves offer a middle ground between aggressive frequency regulation and induced structural loads. When the APC system was augmented with two of the dynamic droop curves considered, grid frequency response was greatly improved over the static droop curve cases. Frequency recovery time, frequency nadir, and steady-state frequency were all improved in two of the dynamic droop curve cases, without inducing oscillations as seen with an aggressive static droop curve. While these dynamic droop curves had the tendency to generally increase individual turbine structural loads compared to a relatively non-aggressive static droop curve, the dynamic droop curves did not generally increase structural loads as much as was observed with the most aggressive static droop curve.

The turbine model used in Section IV to test performance on an individual turbine is the three-bladed Controls Advanced Research Turbine (CART3), located at the National Wind Technology Center. One of the preliminary controllers found in [19] has been tested on the CART3. As the controllers developed in [19] form the basis for the droop curve augmented control systems developed in this study, an area of future work emerged, which is to evaluate the performance of the combined droop curve and APC system developed in this paper on the CART3. In particular, these field tests will be useful in validating the individual turbine simulations and can help confirm the general trend that responding more aggressively to frequency deviations tends to increase structural loads as observed in these simulations.

REFERENCES

[1] "World Wind Energy Report 2010," in *Proc. 10th World Wind Energy Conference*. Cairo, Egypt: World Wind Energy Association, Nov. 2011.

[2] Y. Rebours, D. Kirschen, M. Trotignon, and S. Rossignol, "A Survey of Frequency and Voltage Control Ancillary Services-Part I: Technical Features," in *IEEE Transactions on Power Systems*, vol. 22, no. 1, 2007, pp. 350–357.

[3] E. Ela, M. Milligan, and B. Kirby, "Operating Reserves and Variable Generation," NREL/TP-5500-51928, Tech. Rep., 2011.

[4] J. Aho, A. Buckspan, J. Laks, P. Fleming, F. Dunne, M. Churchfield, L. Pao, and K. Johnson, "A Tutorial of Wind Turbine Control for Supporting Grid Frequency through Active Power Control," in *Proc. American Control Conf.*, Jun. 2012.

[5] A. D. Hansen, "Evaluation of Power Control with Different Electrical and Control Concepts of Wind Farms," Project UpWind, Roskilde, Denmark, Tech. Rep., 2010.

[6] "Wind Farm Transmission Grid Code Provisions: A Direction by the Commission for Energy Regulation," Commission for Energy Regulation, Dublin, Ireland, Tech. Rep., 2004.

[7] "Wind Turbines Connected to Grids with Voltages Above 100kV: Technical Regulation for the Properties and the Regulation for Wind Turbines," Elkraft System and Eltra, Erritsø, Denmark, Tech. Rep., 2003.

[8] "Technical Requirements for the Connection of Generation Facilites to the Hydro-Québec Transmission System: Supplementary Requirements for Wind Generation," Hydro-Québec, Montreal, Québec, Canada, Tech. Rep., 2005.

[9] "Technical Requirements for Wind Power and Photovoltaic Installations and Any Generating Facilities Whose Technology Does Not Consist of a Synchronous Generator Directly Connected to the Grid," Red Electrica, Madrid, Spain, Tech. Rep., 2008.

[10] H. Ma and B. Chowdhury, "Working Towards Frequency Regulation with Wind Plants: Combined Control Approaches," *Renewable Power Generation, IET*, vol. 4, no. 4, pp. 308–316, July 2010.

[11] X. Juankorena, I. Esandi, J. Lopez, and L. Marroyo, "Method to Enable Variable Speed Wind Turbine Primary Regulation," in *International Conference on Power Engineering, Energy and Electrical Drives*, March 2009, pp. 495–500.

[12] I. Gowaid, A. El-Zawawi, and M. El-Gammal, "Improved Inertia and Frequency Support from Grid-Connected DFIG Wind Farms," in *Power Systems Conference and Exposition (PSCE), 2011 IEEE/PES*, Mar. 2011, pp. 1–9.

[13] J. Morren, S. de Haan, W. Kling, and J. Ferreira, "Wind Turbines Emulating Inertia and Supporting Primary Frequency Control," *IEEE Transactions on Power Systems*, vol. 21, no. 1, pp. 433 – 434, Feb. 2006.

[14] M. Liserre, R. Cárdenas, M. Molinas, and J. Rodriguez, "Overview of Multi-MW Wind Turbines and Wind Parks," *IEEE Transactions on Industrial Electronics*, vol. 58, no. 4, pp. 1081–1095, Apr. 2011.

[15] D. Gautam, L. Goel, R. Ayyanar, V. Vittal, and T. Harbour, "Control Strategy to Mitigate the Impact of Reduced Inertia Due to Doubly Fed Induction Generators on Large Power Systems," *IEEE Transactions on Power Systems*, vol. 26, no. 1, pp. 214–224, Feb. 2011.

[16] X. Yuan, J. Chai, and Y. Li, "Control of Variable Pitch, Variable Speed Wind Turbine in Weak Grid Systems," in *IEEE Energy Conversion Congress and Exposition*, Sept. 2010, pp. 3778–3785.

[17] L.-R. Chang-Chien, C.-M. Hung, and Y.-C. Yin, "Dynamic Reserve Allocation for System Contingency by DFIG Wind Farms," *IEEE Transactions on Power Systems*, vol. 23, no. 2, pp. 729–736, May 2008.

[18] R. de Almeida and J. P. Lopes, "Participation of Doubly Fed Induction Wind Generators in System Frequency Regulation," *IEEE Transactions on Power Systems*, vol. 22, pp. 944–950, 2007.

[19] Y. Jeong, "Comparison and Testing of Active Power Control Strategies for Grid-connected Wind Turbines," Master's thesis, Colorado School of Mines, 2011.

[20] J. Jonkman, S. Butterfield, W. Musial, and G. Scott, *Definition of a 5-MW Reference Wind Turbine for Offshore System Development*. Golden, CO: National Renewable Energy Laboratory, Feb. 2009.

[21] A. Yasugi, "Wind Turbine Generator and Method of Controlling the Same," U.S. Patent 0 074 152, Mar. 31, 2011.

[22] A. Nyborg and S. Dalsgaard, "Power Curtailment of Wind Turbines," U.S. Patent 0 286 835, Nov. 11, 2011.

[23] J. Jonkman and M. L. Buhl, *FAST User's Guide*. Golden, CO: National Renewable Energy Laboratory, 2005.

[24] G. Freebury and W. Musial, "Determining Equivalent Damage Loading for Full-Scale Wind Turbine Blade Fatigue Tests," NREL/CP-500-27510, Tech. Rep., 2000.

[25] P. Kundur, N. J. Balu, and M. G. Lauby, *Power System Stability and Control*. New York, NY: McGraw-Hill, 1994.

[26] N. Miller, K. Clark, and M. Shao, "Frequency Responsive Wind Plant Controls: Impacts on Grid Performance," in *2011 IEEE Power and Energy Society General Meeting*, Jul. 2011, pp. 1–8.